Published by the European Association of Geochemistry

Accessory mineral constraints on crustal evolution: elemental fingerprints for magma

**E. Bruand, M. Fowler, C. Storey, O. Laurent, C. Antoine,
M. Guitreau, E. Heilimo, O. Nebel**

Supplementary Information

The Supplementary Information includes:

- Sample Description
- Analytical Techniques
- Tables S-1 to S-3
- Figure S-1
- Supplementary Information References

Sample Description

In this work, we have systematically analysed apatite and titanite (when present) from a range of granitoids from the Archean toward the Phanerozoic (Fig. 1).

TTG and TTG-like

TTG are the main components of Archean cratons and have been interpreted as the results of melted garnet-bearing metabasalt either in subduction or intraplate contexts. They are silica–rich ($SiO_2 > 64$ wt. %), have a high Na_2O content (3-7 wt. %), are low in ferromagnesian, Cr and Ni contents (Moyen and Martin, 2012 and references therein). In this contribution, TTG from different cratons have been studied: Kaapvaal craton (South Africa), Karelia craton (Finland) and the Slave province (Acasta, Canada). In the Kaapvaal craton, the TTG sampled (DWK-04 and HRG-1) are from the Pietersburg block and have been both dated at about 2.9 Ga (Laurent *et al*., 2013). Karelia's samples (EPHE 2004- 369.2 and 413.1) have also been characterised (Mikkola *et al*., 2011) and have been dated at about 2.8 Ga. Acasta samples (AG09-009/14/15 and 16) have previously been characterised for their whole rocks and are dated between 3.9 Ga (AG09-016) and 3.6 Ga (AG09-009/14/15; Guitreau *et al*. 2014; Mojzsis *et al*. 2014). For comparison with those TTG, a TTG-like sample was also analysed. It is an early Permian biotite microgranite from Marie Byrd Land (Antarctica). This sample exposes the same whole rock characteristics as the TTG (high SiO_2, sodic nature, low $K_2O/Na_2O < 0.5$, High Sr >400 and La, low Y; Pankhrust *et al*., 1998) and is therefore belonging to the high-silica adakites group previously defined by Martin *et al*. (2005). Their main petrographic characteristics are compiled in Table S.1. All samples have apatite and zircon as accessory phases. One sample has titanite (EPHE 2004- 369.2) and sample AG09 009 has small grains of primary monazite surrounded by secondary allanite, apatite and grains of thorite (Antoine *et al*., personal communication). All Acasta's samples have clusters of secondary fibrous allanite.

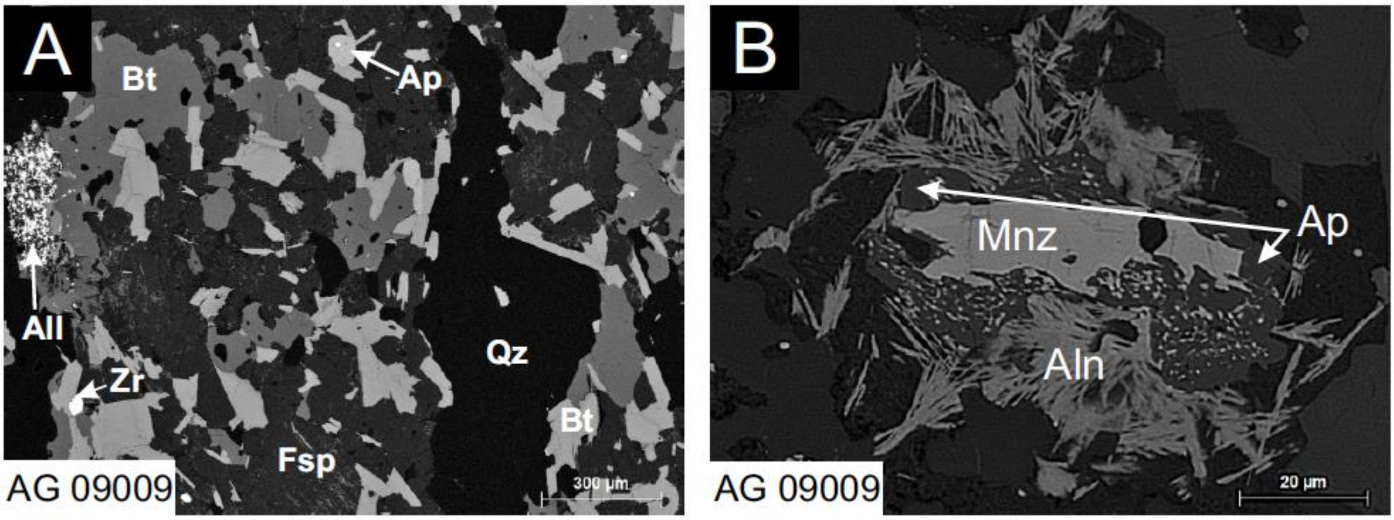

Figure S-1 BSE images of TTG (Acasta) with aggregates of secondary fibrous allanite. Careful study of the samples allowed to find preserved primary monazite partly replaced by secondary allanite, apatite and thorite due to later metamorphic overprinting (Antoine *et al.*, personal communication).

Sanukitoids and High Ba-Sr granite

Sanukitoids are typical magmas appearing at the Archean-Proterozoic transition. Their chemistries have been interpreted as the result of the interaction between a melt or fluid and a mantle wedge. They are chemically characterised by silica contents up to 60 wt. %, Cr > 100 ppm, high Na_2O, K_2O, Sr, Ba and LREE contents (Martin *et al.*, 2005).

Sanukitoids samples in this study are from the Karelia and Kaapvaal cratons. Sanukitoids from Kaapvaal are a granodiorite and a diorite from the Limpopo belt (MAT 43 and MAT 13, Laurent *et* al., 2014a,b, 2017; Laurent and Zeh, 2015) and have been dated around 2.7 Ga. Karelia's samples have also been dated around 2.7 Ga (Heilimo *et al.*, 2011) and are both granodioritic in composition.

The high Ba-Sr suite studied here are the modern equivalent of the sanukitoids (Fowler and Rollinson, 2012). They are Caledonian granitoids that have been characterised for major, trace, Nd ans O isotopes whole rock composition (Fowler *et al.*, 2001; Fowler *et al.*, 2008). The whole-rock chemistry of the selected samples range from granodiorite to granitic compositions. They are located in the northwestern part of Scotland and have been dated at about 425 Ma (Kocks *et al.*, 2014). Description of their mineralogy can be found in Bruand *et al.* (2014). All samples contain apatite, titanite and zircon with some containing allanite or monazite. Trace elements data on accessory phases available in this contribution are from Bruand *et al.* (2014).

Basalt-Andesite-Dacite-Rhyolite (BADR)

The "modern" granitoids samples (BADR samples) studied in this contribution are from the Guernsey igneous complex (Channel Island) which is part of the Armorican massif and is divided geologically into two main parts. The southern part mainly comprises Paleoproterozoic gneisses (The Icartian gneisses; Samson *et al.*, 2003) intruded by syntectonic and subsequently deformed Neoproterozoic granitoids (Perelle quartz-diorite and l'Erée granite; Samson and D'Lemos 1999) and the northern part is dominated by the undeformed, Neoproterozoic Northern Igneous Complex. In order to cover the entire Neoproterozoic plutonic history, samples studied here are from deformed (11-EG-07) and undeformed granitoids (11-BD-02). Sample 11-BD-02 is a diorite while 11-EG-07 is a granodiorite (Table S-1). Plutonic rocks from the Northern Igneous Complex have a calc-alkaline signature and were emplaced at the end of the Cadomian orogeny (*ca.* 560-550 Ma, de Bremond d'Ars *et al.*, 1992). They are referred to by Brown *et al.* (1990) as post-tectonic units. The deformed sample from l'Erée granite (EG-07) in the southern part of the island and its field relationships (e.g. the presence of dykes absent in the north and the presence of foliation) indicate that it belongs to the early Cadomian event and intruded the Icartian basement syntectonically. This is also suggested by age data (Samson et *et al.*, 2003) at 614 Ma +/- 2 Ma. The early Cadomian intrusions in the Channel Islands are calc-alkaline in composition and have typical volcanic arc granites signature (Power *et al.*, 1990). Accessory phases found in the Guernsey igneous complex are apatite, zircon and +/- titanite.

Table S-1 Sample description.

(a)

		Type	Age (Ma)	literature	Comments	Accessories
Kaapvaal craton, South Africa	DWK-04	TTG	2941	Laurent *et al*., 2013; Laurent *et al*, 2014a,b WR	Trondhjemite	apatite, zircon
	HRG-1	TTG	2933		Trondhjemite	apatite zircon
	MAT 13	Sanukitoid	2679	Laurent *et al*., 2013; Laurent *et al*., 2014a,b WR	Granodiorite	apatite, titanite, zircon
Karelia craton, Finland	EPHE 2004 369.2	TTG	2821	Mikkola *et al*., 2011 corresponding sample A1857	Granodiorite	apatite, titanite, zircon, aln
	EPHE 2013 413.1	TTG	2785	Käpyaho *et al*., 2006 corresponding sample A1705	Tonalite	apatite, zircon
	STHA-2009-316	Sanukitoid	2722	Heilimo *et al*., 2011 corresponding sampleA1339	Granodiorite	apatite, titanite, zircon
	A572	Sanukitoid	2723	Heilimo *et al*., 2011	Granodiorite	apatite, titanite, zircon
Marie Byrd Land, Antartica	402-1D	Adakite	early permian	Pankhrust *et al*., 1998	Biotite microgranite	apatite, zircon
High Ba-Sr, Scotland	SR1	Sanukitoid-like	425	Fowler *et al*., 2008; Fowler and Rollinson, 2012	Granodiorite	apatite, titanite, zircon
	SR2	Sanukitoid-like	425		Appinite	apatite, titanite, zircon
	SR3	Sanukitoid-like	425		Granodiorite	apatite, titanite, zircon, aln
	SR4	Sanukitoid-like	425		Granodiorite	apatite, titanite, zircon
	RA1	Sanukitoid-like	425	Kocks *et al*., 2014; Fowler *et al*., 2001, 2008; Fowler and Rollinson, 2012	Appinite	apatite, titanite, zircon
	RT1	Sanukitoid-like	425		Tonalite	apatite, titanite, zircon, aln
	R2	Sanukitoid-like	425		Tonalite	apatite, titanite, zircon, aln
	RGH1	Sanukitoid-like	425		Granite	apatite, titanite, zircon
Slave Province, Acasta, Canada	AG09 009	TTG	3600	Mojzsis *et al*., 2014 for WR and Guitreau *et al*., 2012 for dating	Granitic orthogneiss	apatite, zircon, monazite
	AG09 014	TTG	3600		Tonalitic orthogneiss	apatite, zircon
	AG09 015	TTG	3600		Tonalitic orthogneiss	apatite, zircon
	AG09 016	TTG	3947		Tonalitic orthogneiss	apatite, zircon
Guernsey Igneous Province, Channel Islands	11-BD-02	Arc Magma-Diorite	560-550	Unpublished data in Samson *et al*., (2003)	Bordeaux diorite locality	apatite, titanite, zircon
	11-EG-07	Arc Magma - Granite	614		L'Erée granite locality/granodiorite	apatite, titanite, zircon

(b)

Sample	GPS Coordinates	Sample	GPS Coordinates	Sample	GPS Coordinates
DWK-04[1]	Lat 23.611944S Long 30.328889E	AG09016[3]	Lat 65.160650N Long 115.546033W	SR4[6]	Lat 56.730766N Long 5.540805W
HRG-1[1]	Lat 23.792512S Long 29.127496E	402.1D[4]	Lat 75.00S Long 112.53W	SR3[6]	Lat 56.685100N Long 5.627994W
EPHE 2004 369.2[2]	Lat 65.27511096N Long 29.18714509E	STHA-2009-316[5]	Lat 63.22764732N Long 30.65472253E	SR1[6]	Lat 56.689443N Long 5.602272W

EPHE 2013-413.1[2]	Lat 64.1841557N Long 28.874444 E	A572[5]	Lat 64.44985108N Long 29.00994815E	RT1[6]	Lat 57.993611N Long 4.197395W
AG09009[3]	Lat 65.170217N Long 115.562683W	MAT-13[1]	Lat 23.525368S Long 29.703366E	11-EG-07[7]	Lat 49.454750N Long 2.655250W
AG09014[3]	Lat 65.160250N Long 115.547317W	RHG-1[6]	Lat 58.010645N Long 4.250916W	11-BD-02[7]	Lat 49.490000N Long 2.578361W
AG09015[3]	Lat 65.160250N Long 115.547317W	R2[6]	Lat 57.996508N Long 4.185728W		

[1]Kaapvaal craton, Laurent *et al.* (2014a,b); [2]Karelia craton, Mikkola *et al.* (2011) and Käpyaho *et al.* (2006); [3]Slaves, craton, Mojzsis *et al.* (2006); [4]Byrd Land granitoid, Pankhrust *et al.* (1998); [5]Karelia craton, Heilimo *et al.* (2011); [6]High Ba-Sr, Fowler *et al.* (2008, 2011); [7] Guernsey samples.

Analytical Techniques

The samples were crushed (jaw-crusher, ball mill or Selfrag™), sieved (<355 μm, 355-500 μm and 500-1000 μm fractions) and passed over a Wilfley table. A diamagnetic separator was then used to obtain fractions of different heavy minerals based on their diamagnetic properties. Titanite and apatite were handpicked, mounted in epoxy resin discs and polished for in-situ chemical analysis. Titanite and apatite have also been analysed within thick sections (c. 150 μm).

Image acquisition

Back-scattered electron (BSE) images of titanite were taken with a scanning electron microscope (SEM) JEOL JSM-6100 at the University of Portsmouth (accelerating voltage = 20 kV). Cathodoluminescence (CL) images of apatite were taken with a KeDev Centaurus cathodoluminescence detector housed within a JEOL 6060LV SEM at the University of Portsmouth, or a JEOL JSM-5910 LV with an OPEA detector at the Laboratoire Magmas et Volcans (Clermont-Ferrand, France; accelerating voltage = 15 kV).

Electron probe microanalysis (EPMA)

A Cameca SX-100 microprobe at Bristol University was used for determination of major elements in titanite and zircon using TAP, LPET, PET and LLIF crystals. PC0, TAP, LPET and LLIF crystals were used for apatite. An electron beam of 1 μm was used for titanite and 10 μm for apatite, both with 20 kV accelerating voltage and, 40nA and 10 nA beam currents respectively. An electron beam of 5 μm was used for zircon with an accelerating voltage of 17 kV and a beam current of 100 nA. Several trace elements in these minerals were also analysed for comparison with laser ablation ICP-MS (LA-ICPMS) data. The Durango apatite standard (Marks *et al.*, 2012) and the 91500 zircon standard (Wiedenbeck *et al.*, 2004) were analysed during sessions to monitor data quality.

Trace element analysis : LA-ICPMS

Trace element contents of titanite and apatite were determined by LA-ICPMS at the University of Portsmouth using an Agilent 7500cs (quadrupole) ICPMS and a New-Wave UP213 (λ=213 nm) solid state Nd:YAG laser, or at the Laboratoire Magmas et Volcans (Clermont-Ferrand, France) using an Element XR associated with an excimer laser ATL (Resonetics M-50E; λ = 193 nm). Each analysis consisted of *ca.* 30 s background acquisition and 60 to 80 s sample acquisition. The diameter of the laser beam was 30 μm for titanite and 9-30 μm for apatite.

Internal references used for normalisation of LA-ICPMS data were ^{43}Ca for apatite and titanite and were obtained by EPMA. Details of instruments conditions can be found in Table S-2. Geochemical Data Toolkit (GCDkit, Version 5.0; Janousek *et al.* 2006) was used to plot the data. **All data trace elements on accessory phases and whole rock data presented in this contribution can be found in Table S-3, available for download as an Excel file from http://www.geochemicalperspectivesletters.org/article2006.**

Table S-2 Laser models and conditions to measure apatite and titanite trace elements.

	Frequence	Fluence	Laser Spot	External Standard	Secondary standard analysed during runs
Excimer laser ATL 193 nm Resonetics M-50E with XR Element (Laboratoire Magmas et Volcans)	1-2 Hz	2.8-2.9 J/cm^2	9-12 μm	NIST 610 (Pearce *et al*., 1997) or GSE-1G (Jochum *et al*, 2005)	Durango for Apatite (Marks *et al*., 2013)
New-Wave UP213 (l=213 nm) solid state Nd:YAG laser and 7500 cs Agilent (University of Portsmouth)	10 Hz	4 J/cm^2	30 μm	NIST 610	Durango for Apatite (Marks *et al*., 2013) and in house Khan standard for titanite
Excimer laser S155 Resonetics with Element 2 (Goethe Universitaet Frankfurt)	5 Hz	3-4 J/cm^2	29 μm	NIST 610	Durango

Table S-3 Whole rock analysis and trace elements analysis on apatite and titanite from the different samples studied in this contribution. Chondrite values used for normalisation are from Boynton (1984).

Table S-3 can be downloaded as an Excel file from http://www;geochemicalperspectivesletters.org/article2006.

Supplementary Information References

Boynton, W.V. (1984) Chapter 3 - Cosmochemistry of the Rare Earth Elements: Meteorite Studies. In: Henderson P (ed) *Rare Earth Element Geochemistry*. Elsevier, 63–114

Brown, M., Power, G.M., Topley, C.G., D'Lemos, R.S. (1990) Cadomian magmatism in the North Armorican Massif. *Geological Society of London*, Spec Publ 51,181–213. doi: 10.1144/GSL.SP.1990.051.01.12;

Bruand, E., Storey, C., Fowler, M. (2014) Accessory mineral chemistry of high Ba-Sr granites from Northern Scotland: Constraints on petrogenesis and records of whole-rock Signature. *Journal of Petrology 55,* 1619-1651. doi: 10.1093/petrology/egu037.

De Bremond d'Ars, J., Martin, H., Auvray, B., Lécuyer, C. (1992) Petrology of a magma chamber: the Plutonic Complex of Guernsey (Channel Islands, UK). *Journal of the Geological Society of London* 149, 701–708. doi: 10.1144/gsjgs.150.4.0788;

Fowler, M., Rollinson, H. (2012) Phanerozoic sanukitoids from Caledonian Scotland: Implications for Archean subduction. *Geology* 40, 1079–1082. doi: 10.1130/G33371.1

Fowler, M., Henney, P.J., Darbyshire, D.P.F., Greenwood, P.B. (2001) Petrogenesis of high Ba-Sr granites: the Rogart pluton, Sutherland. *Journal of the Geological Society of London* 158, 521–534. doi: 10.1144/jgs.158.3.521.

Fowler, M., Kocks, H., Darbyshire, D.P.F., Greenwood, P.B. (2008) Petrogenesis of high Ba-Sr plutons from the Northern Highlands Terrane of the British Caledonian Province. *Lithos* 105, 129–148. doi: 10.1016/j.lithos.2008.03.003.

Guitreau, M., Blichert-Toft, J., Martin, H., Mojzsis, S.J., Albarède, F. (2012) Hafnium isotope evidence from Archean granitic rocks for deep-mantle origin of continental crust. *Earth and Planetary Science Letters* 337, 211-223.

Guitreau, M., Blichert-Toft, J., Mojzsis, S.J., Roth, A.S.G., Bourdon, B., Cates, N.L., Bleeker, W. (2014) Lu-Hf isotope systematics of the Hadean-Eoarchean Acasta Gneiss Complex (Northwest Territories, Canada). *Geochimica et Cosmochimica Acta* 135, 251–269. doi: 10.1016/j.gca.2014.03.039.

Heilimo, E., Halla, J., Huhma, H. (2011) Single-grain zircon U-Pb age constraints of the western and eastern sanukitoid zones in the Finnish part of the Karelian Province. *Lithos* 121, 87–99. doi: 10.1016/j.lithos.2010.10.006.

Janousek, V., Farrow, C.M., Erban, V. (2006) Interpretation of Whole-rock Geochemical Data in Igneous Geochemistry : Introducing Geochemical Data Toolkit (GCDkit). *Journal of Petrology* 47, 1255–1259. doi: 10.1093/petrology/egl013;

Jochum, K.P., Willbold, M., Raczek, I., Stoll, B., Herwig, K. (2005). Chemical Characterisation of the USGS Reference Glasses GSA-1G, GSC-1G, GSD-1G, GSE-1G, BCR-2G, BHVO-2G and BIR-1G Using EPMA, ID-TIMS, ID-ICP-MS and LA-ICP-MS. *Geostandards and Geoanalytical Research* 29, 285-302.

Käpyaho, A., Mänttäri, I., Huhma, H. (2006) Growth of Archaean crust in the Kuhmodistrict. Eastern Finland: U–Pb and Sm–Nd isotope constraints on plutonic rocks. *Precambrian Research* 146, 95–119.

Kocks, H., Strachan, R., Evans, J., Fowler, M. (2014) Contrasting magma emplacement mechanisms within the Rogart igneous complex, NW Scotland, record the switch from regional contraction to strike-slip during the Caledonian orogeny. *Geological Magazine* 151, 899–915.

Laurent, O., Paquette, J-L, Martin, H., Doucelance, R. (2013) LA-ICP-MS dating of zircons from Meso- and Neoarchean granitoids of the Pietersburg block (South Africa): Crustal evolution at the northern margin of the Kaapvaal craton. *Precambrian Research* 230, 209–226. doi: 10.1016/j.precamres.2013.02.009.

Laurent, O., Martin, H., Moyen, J.F., Doucelance, R. (2014a) The diversity and evolution of late-Archean granitoids: Evidence for the onset of "modern-style" plate tectonics between 3.0 and 2.5 Ga. *Lithos* 205, 208–235. doi: 10.1016/j.lithos.2014.06.012.

Laurent, O., Rapopo, M., Stevens, G., Moyen, J-F, Martin, H., Doucelance, R., Bosq, C. (2014b) Contrasting petrogenesis of Mg–K and Fe–K granitoids and implications for post-collisional magmatism: Case study from the Late-Archean Matok pluton (Pietersburg block, South Africa). *Lithos* 196–197, 131–149. doi: 10.1016/j.lithos.2014.03.006

Laurent, O., Zeh, A. (2015) A linear Hf isotope-age array despite different granitoid sources and complex Archean geodynamics : Example from the Pietersburg block (South Africa). *Earth and Planetary Science Letters* 430, 326–338. doi: 10.1016/j.epsl.2015.08.028.

Laurent, O., Zeh, A., Gerdes, A., Villaros, A. (2017) How do granitoid magmas mix with each other ? Insights from textures , trace element and Sr – Nd isotopic composition of apatite and titanite from the Matok pluton (South Africa). *Contributions to mineralogy and Petrology* 172, 80 doi: 10.1007/s00410-017-1398-1

Marks, M.A., Wenzel, T., Whitehouse, M.J., Loose, M., Zack, T., Barth, M., Worgard, L., Krasz, V., Eby, G.N., Stosnach, H. (2012) The volatile inventory (F, Cl, Br, S, C) of magmatic apatite: An integrated analytical approach. *Chemical Geology* 291, 241-255.

Martin, H., Smithies, R.H., Rapp, R., Moyen, J-F, Champion, D. (2005) An overview of adakite, tonalite-trondhjemiten-granodiorite (TTG), and sanukitoid: Relationships and some implications for crustal evolution. *Lithos* 79, 1–24. doi: 10.1016/j.lithos.2004.04.048.

Mikkola, P., Huhma, H., Heilimo, E., Whitehouse, M. (2011) Archean crustal evolution of the Suomussalmi district as part of the Kianta Complex, Karelia: Constraints from geochemistry and isotopes of granitoids. *Lithos* 125, 287–307. doi: 10.1016/j.lithos.2011.02.012.

Mojzsis, S.J., Cates, N.L., Caro, G., Trail, D., Abramov, D., Guitreau, M., Blichert-Toft, J., Hopkins, M.D., Bleeker, W. (2014) Component geochronology in the polyphase ca. 3920Ma Acasta Gneiss. *Geochimica Cosmochimica Acta* 133, 68–96. doi: 10.1016/j.gca.2014.02.019.

Moyen, J-F, Martin, H. (2012) Lithos Forty years of TTG research. *Lithos* 148, 312–336. doi: 10.1016/j.lithos.2012.06.010.

Pankhrust, R.J., Weaver, S.D., Bradshaw, J.D., Storey, B.C., Ireland, T.R. (1998) Geochronology and geochemistry of pre-Jurassic superterranes in Marie Byrd Land, Antartica. *Journal of Geophysical Research* 103, 2529–2547.

Pearce, N.J., Perkins, W.T., Westgate, J.A., Gorton, M.P., Jackson, S.E., Neal, C.R., Chenery, S.P. (1997) A compilation of new and published major and trace element data for NIST SRM 610 and NIST SRM 612 glass reference materials. *Geostandards and Geoanalytical Research* 21, 115-144.

Power, G.M., Brewer, T.S., Brown, M., Gibbons, W. (1990) Late Precambrian foliated plutonic complexes of the Channel Islands and La Hague: early Cadomian plutonism. *Geological Society of London*, Spec Publ 51, 215–229. doi: 10.1144/GSL.SP.1990.051.01.13

Samson, S.D., D'Lemos, R.S. (1999) A precise late Neoproterozoic U-Pb zircon age for the syntectonic Perelle quartz diorite, Guernsey, Channel Islands, UK. *Geological Society of London* 156, 47–54. doi: 10.1144/gsjgs.156.1.0047

Samson, S.D., D'Lemos, R.S., Blichert-Toft, J., Vervoort, J. (2003) U-Pb geochronology and Hf-Nd isotope compositions of the oldest Neoproterozoic crust within the Cadomian orogen: New evidence for a unique juvenile terrane. *Earth and Planetary Science Letters* 208, 165–180. doi: 10.1016/S0012-821X(03)00045-1